

**Fig. 3.** Renal survival of immunoglobulin A nephropathy (IgAN) patients with or without hypertension at the time of diagnosis. In the patients with hypertension, the PPAR $\gamma$  gene (*PPARG*) C161T polymorphism did not affect the renal survival [(a), Kaplan-Meier, Log rank test,  $p=0.3912$ ]. However, the polymorphism had an influence on the renal survival in the patients without hypertension [(b), Kaplan-Meier, Log rank test,  $p=0.0240$ ]. ESRD, end-stage renal disease.

in patients with CAD (23), similar to that seen in IgAN patients in the present study. The mechanisms whereby the C161T polymorphism, located at exon 6 of *PPAR*, affects the renal survival rate of IgAN are not yet determined. The polymorphism did not affect the histological changes, at least, at the time of diagnosis when the renal biopsy was performed. As this nucleotide polymorphism does not result in an amino acid substitution, other functional gene polymorphisms, which are in linkage disequilibrium with this polymorphism, may be responsible for determining the renal survival of IgAN patients. The findings in the present and the previous study (23) may suggest that the *PPARG* C161T polymorphism is independent of the functions of this gene product, which are related to lipid metabolism, obesity, and hypertension.

Interestingly, the renal prognosis of the IgAN patients with hypertension was not affected by the polymorphism, suggesting that the impact of hypertension on the progression of renal diseases might mask the influence of the polymorphism in the subgroup with hypertension. The possible mechanisms responsible for this might be, for example; (1) The change in the renal hemodynamics induced by hypertension might affect the function of PPAR $\gamma$  in kidney cells, and (2) the difference in insulin resistance linked to the polymorphism does not influence the renal prognosis because hypertensive patients are often highly resistant to insulin, possibly through pathways other than PPAR $\gamma$  (26). However, no direct evidence for these mechanisms was shown in this study.

In summary, we identified the T allele of *PPARG* C161T polymorphism as a predictor of renal survival in IgAN patients without hypertension. Although a large prospective study may be needed to test the present observations, the results of this study, if confirmed, may suggest that the compounds which control the functions of PPAR $\gamma$  such as antidiabetic thiazolidinediones

could be applied as new therapeutic agents for IgAN.

### Acknowledgements

This work was supported by a Health and Labour Science Research Grants for Research on Specific Diseases from the Ministry of Health, Labour and Welfare, and by a grant-in-aid for Scientific Research (No. 11671032 and 12670420) from the Ministry of Education, Culture, Sports, Science and Technology of Japan. We gratefully acknowledge the excellent technical assistance of Noriko Ikeda and Kumiko Furui.

### References

- Galla JH. IgA nephropathy. *Kidney Int* 1995; 47 (2): 377-387.
- Koyama A, Igarashi M, Kobayashi M. Natural history and risk factors for immunoglobulin A nephropathy in Japan. Research Group on Progressive Renal Diseases. *Am J Kidney Dis* 1997; 29 (4): 526-532.
- Levy M, Berger J. Worldwide perspective of IgA nephropathy. *Am J Kidney Dis* 1988; 12 (5): 340-347.
- Szeto CC, Lai FM, To KF et al. The natural history of immunoglobulin A nephropathy among patients with hematuria and minimal proteinuria. *Am J Med* 2001; 110 (6): 434-437.
- Hsu S, Ramirez S, Winn M et al. Evidence for genetic factors in the development and progression of IgA nephropathy. *Kidney Int* 2000; 57 (5): 1818-1835.
- Rantala I, Mustonen J, Hurme M et al. Pathogenetic aspects of IgA nephropathy. *Nephron* 2001; 88 (3): 193-198.
- Scolari F, Amoroso A, Savoldi S et al. Familial clustering of IgA nephropathy: further evidence in an Italian population. *Am J Kidney Dis* 1999; 33 (5): 857-865.
- Alamartine E, Sabatier JC, Guerin C et al. Prognostic factors in mesangial IgA glomerulonephritis: an extensive study with univariate and multivariate analyses. *Am J Kidney Dis* 1991; 18 (1): 12-19.
- Issemann I, Green S. Activation of a member of the steroid hormone receptor superfamily by peroxisome proliferators. *Nature* 1990; 347 (6294): 645-650.
- Guan Y, Breyer MD. Peroxisome proliferator-activated receptors (PPARs): novel therapeutic targets in renal disease. *Kidney Int* 2001; 60 (1): 14-30.
- Clark RB. The role of PPARs in inflammation and immunity. *J Leukoc Biol* 2002; 71 (3): 388-400.

### *PPARG C161T polymorphism in IgA nephropathy*

12. Elangbam CS, Tyler RD, Lightfoot RM. Peroxisome proliferator-activated receptors in atherosclerosis and inflammation—an update. *Toxicol Pathol* 2001; 29 (2): 224–231.
13. Chinetti G, Fruchart JC, Staels B. Peroxisome proliferator-activated receptors (PPARs): nuclear receptors at the crossroads between lipid metabolism and inflammation. *Inflamm Res* 2000; 49 (10): 497–505.
14. Ma LJ, Marcantoni C, Linton MF et al. Peroxisome proliferator-activated receptor-gamma agonist troglitazone protects against nondiabetic glomerulosclerosis in rats. *Kidney Int* 2001; 59 (5): 1899–1910.
15. Buckingham RE, Al-Barazanji KA, Toseland CD et al. Peroxisome proliferator-activated receptor-gamma agonist, rosiglitazone, protects against nephropathy and pancreatic islet abnormalities in Zucker fatty rats. *Diabetes* 1998; 47 (8): 1326–1334.
16. Natarajan C, Bright JJ. Peroxisome proliferator-activated receptor-gamma agonists inhibit experimental allergic encephalomyelitis by blocking IL-12 production, IL-12 signaling and Th1 differentiation. *Genes Immun* 2002; 3 (2): 59–70.
17. Oates JC, Reilly CM, Crosby MB et al. Peroxisome proliferator-activated receptor agonists: Potential use for treating chronic inflammatory diseases. *Arthritis Rheum* 2002; 46 (3): 598–605.
18. Yang XY, Wang LH, Chen T et al. Activation of human T lymphocytes is inhibited by peroxisome proliferator-activated receptor gamma (PPARgamma) agonists. PPAR-gamma co association with transcription factor NFAT. *J Biol Chem* 2000; 275 (7): 4541–4544.
19. Delerive P, Fruchart JC, Staels B. Peroxisome proliferator-activated receptors in inflammation control. *J Endocrinol* 2001; 169 (3): 453–459.
20. Shiomi T, Tsutsui H, Hayashidani S et al. Pioglitazone, a peroxisome proliferator-activated receptor-gamma agonist, attenuates left ventricular remodeling and failure after experimental myocardial infarction. *Circulation* 2002; 106 (24): 3126–3132.
21. Fajas L, Fruchart JC, Auwerx J. PPAR $\gamma$ 3 mRNA: A distinct PPAR $\gamma$  mRNA subtype transcribed from an independent promoter. *FEBS Lett* 1998; 438: 55–60.
22. Zhu Y, Qi C, Korenberg JR et al. Structural organization of mouse peroxisome proliferator-activated receptor gamma (mPPAR gamma) gene: alternative promoter use and different splicing yield two mPPAR gamma isoforms. *Proc Natl Acad Sci USA* 1995; 92 (17): 7921–7925.
23. Wang XL, Oosterhof J, Duarte N. Peroxisome proliferator-activated receptor gamma C161  $\rightarrow$ T polymorphism and coronary artery disease. *Cardiovasc Res* 1999; 44 (3): 588–594.
24. Suzuki S, Sato H, Kobayashi H et al. Comparative study of IgA nephropathy with acute and insidious onset. Clinical, laboratory and pathological findings. *Am J Nephrol* 1992; 12 (12): 22–28.
25. Takano H, Komuro I. Roles of peroxisome proliferator-activated receptor gamma in cardiovascular disease. *J Diabetes Complications* 2002; 16 (1): 108–114.
26. Imazu M. Hypertension and insulin disorders. *Curr Hypertens Rep* 2002; 4 (6): 477–482.

## Cloning and characterization of a novel gene promoting ureteric bud branching in the metanephros<sup>1</sup>

TAKASHI ARAKI, MATSUHIKO HAYASHI, and TAKAO SARUTA

Department of Internal Medicine, Keio University School of Medicine, Tokyo, Japan

### Cloning and characterization of a novel gene promoting ureteric bud branching in the metanephros.

**Background.** The ureteric buds and metanephric mesenchymal cells reciprocally induce each other's maturation during kidney development, and implicated transcription factors, secreted growth factors, and cell surface signaling peptides are critical regulators of renal branching morphogenesis. Protein kinase C (PKC) is a key enzyme in the signal transduction mechanisms in various biologic processes, including development, because it regulates growth and differentiation. Inhibition of PKC by the sphingolipid product ceramide interferes with nephron formation in the developing kidney, but the molecule that controls ureteric bud branching downstream of PKC is still unknown.

**Methods.** Differential display polymerase chain reaction (PCR) of metanephroi cultured with a PKC activator and inhibitor was performed. We also examined the role of a novel gene in kidney development with organ culture system.

**Results.** A novel gene encoding a 759 bp mRNA was identified, and we named it metanephros-derived tubulogenic factor (*MTF*)/*L47*. Inhibition of *MTF* with antisense oligonucleotide impaired ureteric bud branching by cultured metanephroi, and addition of recombinant *MTF* protein promoted ureteric bud branching in cultured metanephroi and increased cell proliferation.

**Conclusion.** We identified a novel molecule in developing kidney that is capable of modulating ureteric bud branching and kidney differentiation.

Ureteric bud branching is one of the most important processes in renal organogenesis, and reciprocal induction by ureteric bud and metanephric mesenchymal cells is important for ureteric bud branching and mesenchyme-to-epithelial conversion [1]. Undifferentiated metanephric mesenchymal cells are rescued from programmed cell death by a signal from the ureteric buds, condense around the tip of the ureteric buds, become po-

larized epithelium, and form vesicles. The vesicles then elongate and differentiate to form the proximal nephron in the kidney. The ureteric buds are in turn rescued from degeneration by the signal from nephrogenic and stromal progenitor mesenchyme, branch, and then elongate to form collecting ducts.

In signal transduction mechanisms in various biologic processes and in controlling gene expression during organ development, protein kinase C (PKC), a serine/threonine kinase, is recognized as a key enzyme [2, 3]. In addition, it is involved in the regulation of growth and differentiation during development. Kidney development is governed by proliferation, differentiation, and apoptosis. Several isoforms of PKC are expressed during kidney development, and inhibition of PKC by a sphingolipid product, ceramide, interferes with nephron formation (poor branching of ureteric buds) and induces apoptosis in the developing kidney [4]. However, since the molecule that promotes ureteric bud branching downstream of PKC was unknown, we performed differential display of PKC-activated metanephros and PKC-inhibited metanephros to access a new gene that controls ureteric bud branching downstream of PKC.

The metanephros-derived tubulogenic factor (*MTF*) gene was originally identified as part of a technique in an mRNA differential display project designed to identify genes up-regulated by PKC activation in kidney organ culture. Subsequent cloning and sequencing of the full-length cDNA revealed a sequence with homology to the previously reported human CGI-204 cDNA. We examined the role of this novel gene during renal development by using antisense oligonucleotides and recombinant protein in a metanephric organ culture system.

This study investigated a novel gene, *MTF*, that promotes ureteric bud branching in kidney organ cultures downstream of PKC.

### METHODS

#### Kidney organ culture

Kidney organ culture was established from mouse embryo as described previously. Embryos were dissected

<sup>1</sup>See Editorial by Nigam, p. 2320.

**Key words:** metanephros, PKC, ureteric bud branching, cell proliferation.

Received for publication February 4, 2003  
and in revised form May 31, 2003  
Accepted for publication July 17, 2003

© 2003 by the International Society of Nephrology

from 12 dpc ICR mice. Metanephroi and associated ureteric buds were microdissected en bloc and cultured on polycarbonate filters (pore size, 1.0  $\mu\text{m}$ ) (Nuclepore, Pleasanton, CA, USA) in serum-free Ham's F12:Dulbecco's modified Eagle's medium (DMEM) 1:1 (Invitrogen, Carlsbad, CA, USA) medium with the supplements described [5]. After adding the PKC activator 5 nmol/L phorbol 12-myristate 13-acetate (PMA) or the PKC inhibitor 100  $\mu\text{mol/L}$  *N*-acetyl-D-sphingosine (C2 ceramide) to the medium, and culturing for 72 hours, the metanephroi were used in the experiments described below.

#### Evaluation of ureteric bud branching and tubule induction

To visualize ureteric bud growth, cultured whole metanephroi were fixed with cold methanol for 10 minutes, washed three times with phosphate-buffered saline (PBS) with bovine serum albumin (BSA) (PBST), and incubated overnight at 4°C with monoclonal antipancytokeratin antibody (1:50 dilution) (Sigma Chemical Co., St. Louis, MO, USA). After washing samples PBST three times, they were incubated with Cy3-labeled antimouse IgG (PA) (1:50 dilution) (Jackson Immuno Research West Grove, PA, USA), again washed with PBST three times, and examined with a fluorescence microscope. The degree of branching morphogenesis of the developing ureteric bud was assessed by counting the number of terminal ampullae as described by Li et al [6]. To visualize tubule formation, fixed metanephroi were incubated with fluorescein isothiocyanate (FITC)-conjugated LT (*Lotus tetragonolobus*) lectin (1:50 dilution) (Funakoshi, Tokyo, Japan) for 180 minutes at room temperature. Samples were washed with PBST three times, mounted, and examined.

#### Differential display

TRizol Reagent (Invitrogen) was used to isolate total RNA from metanephroi treated with PMA or C2 ceramide for 72 hours, and it was exposed to DNase (Takara, Shiga, Japan). After reverse transcription with oligo-dT primer (mRNA finger printing kit; Nippon Gene, Tokyo, Japan), an arbitrary primed polymerase chain reaction (PCR) was carried out with oligo-dT primer and arbitrary primers. The thermocycle conditions were: one cycle of 3 minutes at 95°C, 5 minutes at 40°C, and 5 minutes at 72°C; 24 cycles of 15 seconds at 95°C, 2 minutes at 40°C, and 1 minute at 72°C; and 5 minutes at 72°C. The PCR products were separated by a 2% agarose gel electrophoresis and stained with ethidium bromide. Differentially expressed bands were excised from the gel, eluted, and reamplified by PCR under conditions following the procedure described by the supplier. Reamplified PCR products were subcloned into pT7 Blue vector

(Novagen, Madison, WI, USA) with the ligation high (Toyobo, Tokyo, Japan) and then sequenced. The arbitrary primer that yielded a different band of PCR product was 5-GATCGCATTG-3.

#### Full-length cDNA cloning and sequencing

We utilized a mouse est cDNA database to estimate the full-length cDNA based on the 290 bp mouse cDNA fragment generated by differential display. A 759 bp full-length cDNA was suspected, and we performed reverse transcription (RT)-PCR with mouse embryonic kidney mRNA with the following primers to obtain it: forward, 5'-ATGGCTGCGACCAGTCTAGTGGGTA TT-3' (MTF-f); reverse, 5'-GACACTACTTGATTTC GTTCTTGAGA-3' (MTF-r). The PCR product was cloned into pT7 Blue vector (named MTF/pT7Blue) and sequenced.

#### RT-PCR and Northern hybridization

After incubating 1  $\mu\text{g}$  of total RNA from the metanephroi of 12 dpc and 16 dpc mouse or neonatal and adult mouse kidney with RNase-free DNase, and it was reverse transcribed into cDNA with random primers and Moloney-murine mouse virus (Mo-MLV) reverse transcriptase (Invitrogen). The reaction mixture contained 9 pmol random deoxynucleotide hexamers, 1 $\times$  reverse transcription buffer, 6.7 mmol/L dithiothreitol (DTT), 0.624 mmol/L desoxynucleoside triphosphate (dNTP), 0.8 units of RNase-OUT, and 4 units Mo-MLV reverse transcriptase. The reaction was allowed to proceed at 37°C for 90 minutes, and the cDNA synthesized was used for PCR. The primers used for developmental RT-PCR were MTF-f and MTF-r, and they amplified a 759 bp PCR product. The amplification was performed in a thermal cycler and included 1-minute denaturing at 95°C, 1-minute annealing at 56°C, and 1-minute extension at 72°C. The PCR was run for 28 cycles for MTF/L47 and 23 cycles for  $\beta$ -actin.

The filter for Northern hybridization was purchased from Clontech (Multiple Tissue Northern Blots, Mouse MTN Blot; Clontech, Palo Alto, CA, USA) and was hybridized to the probe made with the EcoRI/SalI MTF/pT7 Blue fragment. The Clontech Multiple Tissue Northern Blots contained oligo-dT-purified mRNA from different specific normal mouse tissues. The probe was hybridized to the filter at 62°C overnight, and after washing the filter twice with wash solution, BAS 5000 was exposed to it for 60 minutes. After stripping, the same filter was hybridized to the  $\beta$ -actin probe.

#### TaqMan PCR

Total RNA was extracted from cultured metanephroi with TRizol reagent. Single-strand DNA was generated

from the RNA by using the TaqMan Reverse Transcription Reagents (Applied Biosystems, Foster City, CA, USA), and the product was used as a template for real-time PCR by using the ABI Prism 7700 Sequence Detection System (Perkin-Elmer Applied Biosystems). Expression of MTF/L47 mRNA was quantitatively determined by using the TaqMan Universal Master Mix (Applied Biosystems) according to the manufacturer's instructions, and standardization was achieved by using rRNA representation. The primers and TaqMan probe were designed using the Perkin-Elmer computer program Primer Express. The forward primer for MTF was GTGCTTGGAGAAGGGACATCT, and the reverse primer was GAACCGCCTCCTGTTGTAT. The probe was FAM-TCTGGCACAAATTCAAGCAG TGGCCTAT. A 50 ng sample of total RNA was used per reaction, and TaqMan ribosomal RNA Control Reagents (Perkin-Elmer Applied Biosystems) were used as internal controls for mRNA expression.

#### In situ hybridization

For in situ hybridization, metanephroi of 16 dpc mice were fixed in 4% paraformaldehyde and embedded in 22-oxacalciol (OCT) compound (Tissue-Tek, Milano, Italy). Frozen samples were then cut into 6  $\mu$ m thick sections, and the sections were hybridized with cRNA probes. The cRNA probes were labeled with digoxigenin and detected with a digoxigenin detection kit (Boehringer Mannheim, Mannheim, Germany) according to the manufacturer's instructions.

#### Antisense S-oligonucleotide

To investigate the role of MTF/L47 in kidney development, a 20mer antisense S-oligonucleotide (S-ODN) of MTF/L47, designed to include the first ATG and scramble S-ODN, were added to organ cultures. Media containing S-ODNs were prepared by adding 32  $\mu$ L of LipofectAmine (Invitrogen) and an antisense S-ODN or a scramble S-ODN to 40  $\mu$ L of Opti-MEM (Invitrogen) to give a final concentration of 8  $\mu$ mol/L S-ODN in 800  $\mu$ L, and then incubating for 45 minutes at room temperature. The S-ODN/LipofectAmine mixture was then added to the culture medium to give a final volume of 800  $\mu$ L. After 24 hours, the growth medium was replaced with fresh mixtures prepared as described previously. After 72 hours, cultured metanephroi were analyzed by immunohistochemistry and RT-PCR.

#### Synthesize of recombinant protein

RT-PCR was performed for cloning MTF/L47 cDNA into expressional vector pCDNA 3.1 HisA (Invitrogen). The primers were: forward, 5'-CATATGGATCCTGGCTGCGAC-3' and reverse, 5'-GGGGACTCGAGTGA CACTACT-3'. The PCR product was digested with BamHI and XhoI, and the fragment was cloned into

pCDNA 3.1 HisA. MTF/L47 was expressed in a coupled in vitro transcription-translation system using the TnT-T7 Reticulocyte Lysate System (Promega) by following the procedure described by the supplier. A 1  $\mu$ g amount of plasmid DNA was used in the 50  $\mu$ L assay. The reaction mixture was incubated at 30°C for 90 minutes.

#### Detection of apoptosis

Apoptotic cells in cultured metanephroi were detected by a TUNEL method (DeadEnd Fluorometric TUNEL System; Promega). Cultured metanephroi were fixed and embedded in OCT compound (Tissue-Tek) as described previously [5]. Frozen samples were cut into 6  $\mu$ m thick sections, and the sections were incubated with equilibration buffer for 10 minutes at room temperature and then at 37°C for 60 minutes with working-strength terminal deoxynucleotidyl transferase (TdT) reaction buffer. The reaction was stopped by incubation for 10 minutes in 2 $\times$  standard sodium citrate (SSC). After washing with PBS, the sections were incubated with Hoechst 33342 (10  $\mu$ mol/L) to visualize the nuclei.

#### [<sup>3</sup>H]-thymidine incorporation studies

Metanephroi were cultured for 24 hours with or without recombinant MTF/L47 protein, and then exposed to 25  $\mu$ Ci/mL [<sup>3</sup>H]-thymidine for 24 hours. Explants were washed with cold PBS twice and treated with 5% trichloroacetic acid for 30 minutes at 90°C [7]. The hydrolysates were centrifuged, and the supernatants were counted with a liquid scintillation counter.

## RESULTS

#### PKC activation promotes ureteric bud branching

C2 ceramide inhibited ureteric bud branching in organ culture as in the previous report, and PMA promoted it (Fig. 1).

#### Cloning of MTF/L47

We obtained 20 fragments by the differential display method, one of which was the KIAA0266 gene product, and another was the aspartate aminotransferase gene. We identified a 290 bp product that showed sequence identity to a mouse est database clone. The est search revealed a 759 bp full-length cDNA with homology to human CGI-204. To obtain the full-length cDNA of mouse MTF/L47, we performed RT-PCR of mouse embryonic kidney mRNA with primers MTF-f and MTF-r, and a 759 bp PCR product with a sequence identical to that in the est data base was obtained, and we named it MTF. MTF/L47 showed high homology to human CGI-204, and the amino acid homology was 86% (Fig. 2). MTF/L47 showed homology to drosophilla R1c1, with 46% amino acid homology.

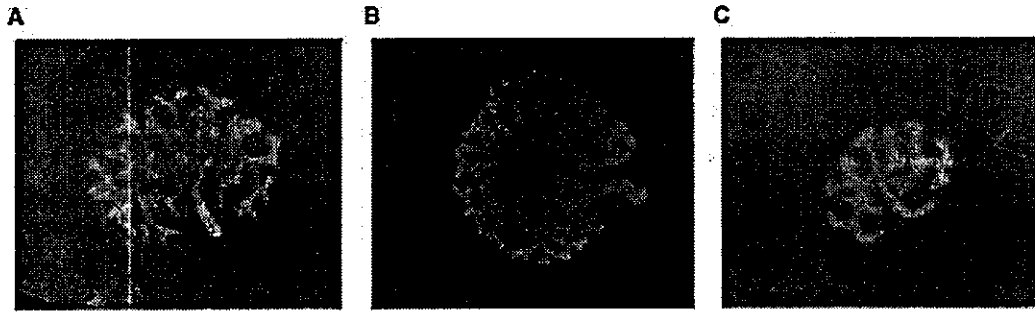


Fig. 1. Ureteric bud branching in protein kinase C (PKC)-activated and -inhibited cultured metanephros. (A) Control. (B) Exposure to 5 nmol/L phorbol 12-myristate 13 acetate (PMA) promoted ureteric bud branching of cultured metanephroi. (C) Exposure to 100 μmol/L C2 ceramide inhibited ureteric bud branching in organ culture.

Mouse	1	MAATSLVIGICRRASAFLLKAAACSLVNPKDAAHSGCRSSLSLLHKNTPHVTS
Human	1	MAATSLVIGICRRASAFLLKAAACSLVNPKDAAHSGCRSSLSLLPKSTPNVTS
Mouse	51	FLGCKLLHTLSRKGLEEFFDDPKNWGEEKVKSAGASWTQQGLRNKSNEDL
Human	51	FHQYRLHTLSRKGLEEFFDDPKNWGEEKVKSAGAAWTQQGLRNKSNEDL
Mouse	101	HKLWYVLLKERNMLLTLEQEAQRQLPWPSPERLEKVVDSMDNVDRVVQE
Human	101	HKLWYVLLKERNMLLTLEQEAQRQLPWPSPERLDKVVDSMDALDKVVQE
Mouse	151	REDALRLQLTGQEKPRPGAWRRDIFGRIVVHKFKQWPIPWYLNKRYNRRR
Human	151	REDALRLQLTGQERARPGAWRRDIFGRIVVHKFKQWPIPWHLNKRYNRRR
Mouse	201	FFAMPYVDRFIRL-RIEKHARIEARKRSLQKKKEKILHAKPFLSQER-K
Human	201	FFALPYVDHFLRLER-EKRARKKARKENLERKAKILLKKPFLA-EAGK
Mouse	251	SSSV
Human	251	SSLV

Fig. 2. Deduced amino acid sequence of mouse metanephros-derived tubulogenic factor (MTF/L47). The amino acid sequence of mPOM210 is available from EMBL/GenBank/DBJ under accession number XP.130843. The human homologue (CGI-204) sequence (EMBL/GenBank/DBJ accession number AAG01157) is written below the mouse sequence. Human amino acid residues identical to the mouse residues are shown as dots.

**MTF/L47 was increased in cultured PKC-activated metanephroi**

To confirm that MTF/L47 was regulated by PKC in cultured metanephroi, we performed an RT-PCR analysis with PMA-treated cultured metanephroi and C2 ceramide-treated cultured metanephroi. The increased expression of MTF/L47 mRNA in PMA-treated metanephroi was quantitatively confirmed by the laser microdissection method (LMM) along with real-time PCR analysis. The level of MTF/L47 mRNA was greater in the PMA-treated metanephroi than in C2 ceramide-treated metanephroi (1.64 ± 0.32 vs. 0.81 ± 0.11 expression ratio, control was 1.03 ± 0.20, N = 3) (Fig. 3).

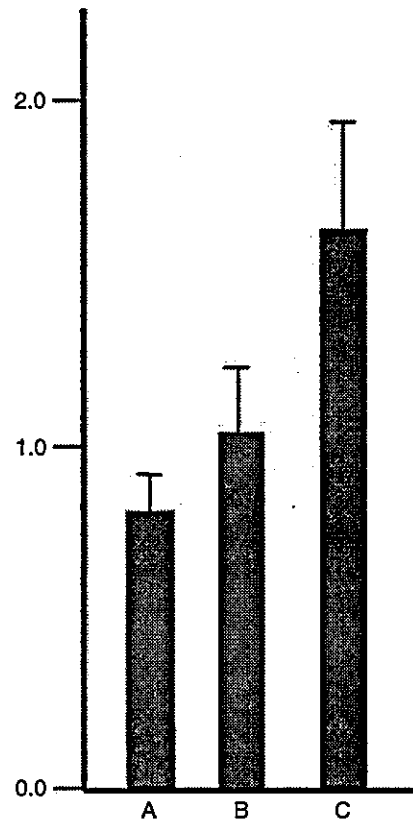
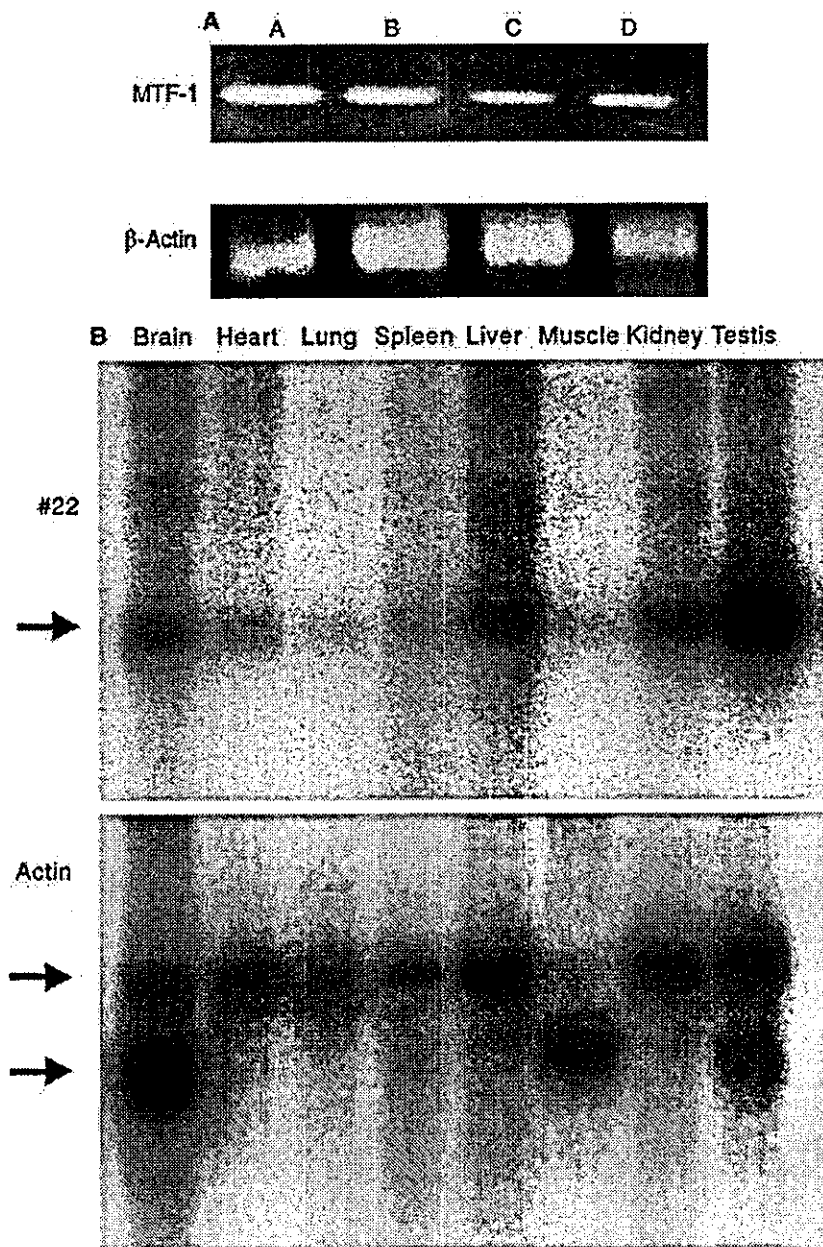


Fig. 3. Mouse metanephros-derived tubulogenic factor (MTF/L47) expression in protein kinase C (PKC)-activated and -inhibited cultured metanephros. TaqMan reverse transcription-polymerase chain reaction (RT-PCR) analysis revealed a higher MTF/L47 expression ratio to rRNA in phorbol 12-myristate 13 acetate (PMA)-treated cultured metanephroi than in C2 ceramide-treated cultured metanephroi (N = 3). (A) Exposure to PMA. (B) Control. (C) Exposure to C2 ceramide.

**Developmental expression of MTF/L47 in mouse kidney**

Gene expression of MTF/L47 was investigated in mouse kidney by RT-PCR at various stages of development. Strong MTF/L47 expression was observed on E12 and E16, and it was weaker in neonatal and adult kidney



**Fig. 4.** Analysis of expression of mouse metanephros-derived tubulogenic factor (*MTF/L47*) by reverse transcription-polymerase chain reaction (RT-PCR), Northern blotting, and in situ hybridization. (A) RT-PCR analysis of expression of *MTF/L47* in fetal and postnatal mouse kidney. Strong *MTF/L47* expression was observed on E12 and E16, and was weaker in neonatal and adult kidney. Lane A, E12; lane B, E16; lane C, P0; and lane D, adult. (B) Tissue distribution of *MTF/L47* mRNA in adult mouse detected by Northern blotting. Expression of *MTF/L47* was high in the testis, brain, liver, and kidney. (C) In situ hybridization analysis revealed that *MTF/L47* was expressed mainly in tubules in the medulla, and it was not expressed in developing nephrons.

(Fig. 4A), suggesting that *MTF/L47* is developmentally regulated.

#### In situ hybridization of *MTF/L47*

Localization of *MTF/L47* was restricted to the tubule-forming cells, and it was not detected in developing glomeruli (Fig. 4C).

#### Tissue distribution of *MTF/L47* mRNA in adult mice

Several mouse tissues were examined for *MTF/L47* mRNA expression by Northern blotting. A single ~1.0 kbp mRNA transcript was observed on some tis-

sues. Expression of *MTF/L47* was high levels in the testis, brain, liver, and kidney (Fig. 4B). Low level expression was found in the lung, muscle, spleen, and heart.

#### Role of *MTF/L47* in mammalian metanephrogenesis

We then proceeded to investigate the role of *MTF/L47* in metanephric development by utilizing antisense S-ODN and the organ culture system. The metanephroi of the explants exposed to antisense S-ODN for 72 hours exhibited marked changes. There was an overall reduction in the size of the explants and a marked reduction in ureteric bud branching (Fig. 5A). By contrast, there

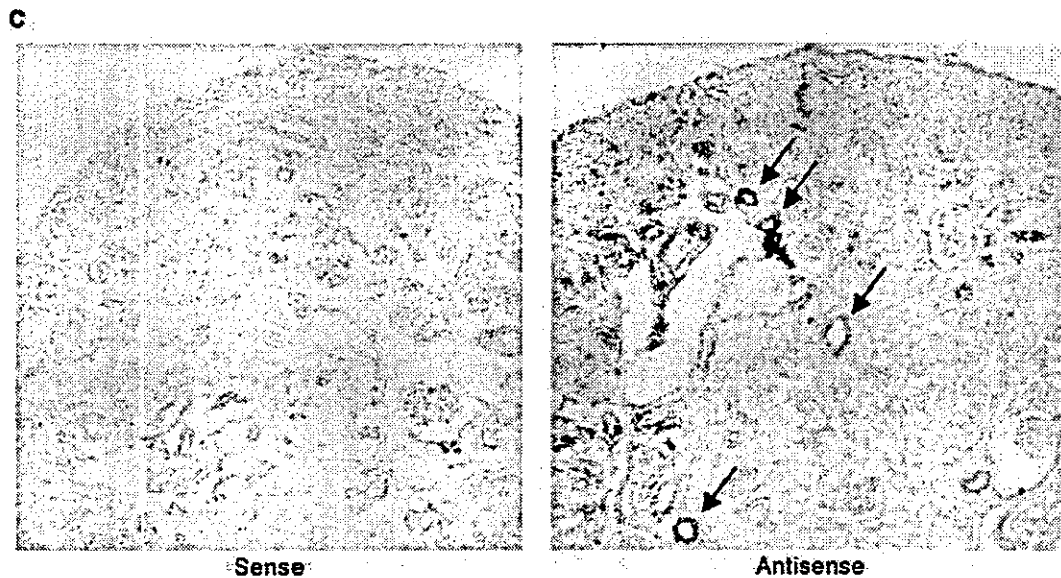


Fig. 4. (Continued)

were no differences between scramble S-ODN-treated metanephroi and control-cultured metanephroi in size or ureteric bud branching (Fig. 5A). We performed TaqMan RT-PCR analysis to confirm that the inhibition of ureteric bud branching was attributable to antisense S-ODN, and results showed less MTF/L47 mRNA in the antisense S-ODN-treated metanephroi than in the scramble ODN-treated metanephroi ( $0.28 \pm 0.13$  vs.  $1.22 \pm 0.39$  expression ratio,  $N = 3$ ) (Fig. 5B).

Next, we used the recombinant MTF/L47 protein to investigate the role of MTF/L47 in metanephric development in greater detail. The explants exposed to recombinant MTF/L47 protein for 72 hours exhibited increased ureteric bud branching (Fig. 6) and increased LT-lectin-positive structures (Fig. 6). The number of ampullae increased from  $33.7 \pm 3.5$  (control) to  $48.7 \pm 2.5$  (recombinant protein) in response to the recombinant protein ( $N = 3$ ). We used nonincubated reticulocyte lysate as a control to eliminate the influence of the reticulocyte lysate, and the number of LT-lectin-positive structures increased 1.3 times in response to the recombinant protein over the control.

#### Apoptosis of recombinant MTF/L47 protein-treated metanephroi

Because the recombinant protein-treated metanephroi were larger than the control metanephroi, we performed the TUNEL assay, which stains apoptotic cells with fluorescein-labeled deoxyuridine triphosphate (dUTP). After 72 hours in culture, metanephroi that have been exposed to recombinant protein and reticulocyte lysate were embedded and frozen sectioned. The TUNEL assay revealed apoptotic cells among undifferentiated mes-

enchymal cells, but no significant difference was found between control and recombinant protein (Fig. 7).

#### Cell proliferation of recombinant MTF/L47 protein-treated metanephroi

Since there was no difference in apoptosis between the recombinant MTF/L47-treated metanephroi and the controls, we investigated [ $^3$ H]-thymidine-associated incorporation by cultured metanephroi. The total [ $^3$ H]-thymidine-associated radioactivity incorporated in the whole explants was greater in the MTF/L47 recombinant protein-treated kidneys than in the controls ( $11343 \pm 2412$  vs.  $18577 \pm 6741$  cpm/metanephros,  $N = 18$ ) (Fig. 8).

#### DISCUSSION

Cell proliferation, motility, differentiation, and extracellular matrix production are all critical events during embryonic tissue development. Metanephric kidney development is characterized by epithelial cell growth and differentiation from ureteric buds and induction of the surrounding mesenchymal cells. Several soluble growth factors, including hepatocyte growth factor (HGF) [8–11], glial cell-derived neurotrophic factor (GDNF) [12], insulin-like growth factors (IGFs) [13, 14], epidermal growth factors (EGFs) [15, 16], fibroblast growth factor (FGF) [17], and bone morphogenetic protein-7 (BMP-7) [18], have been thought to be involved in the mesenchymal-to-epithelial conversion and branching morphogenesis of ureteric buds. Phosphorylation events are considered to play crucial roles in determining the degree of tubule formation during the early development



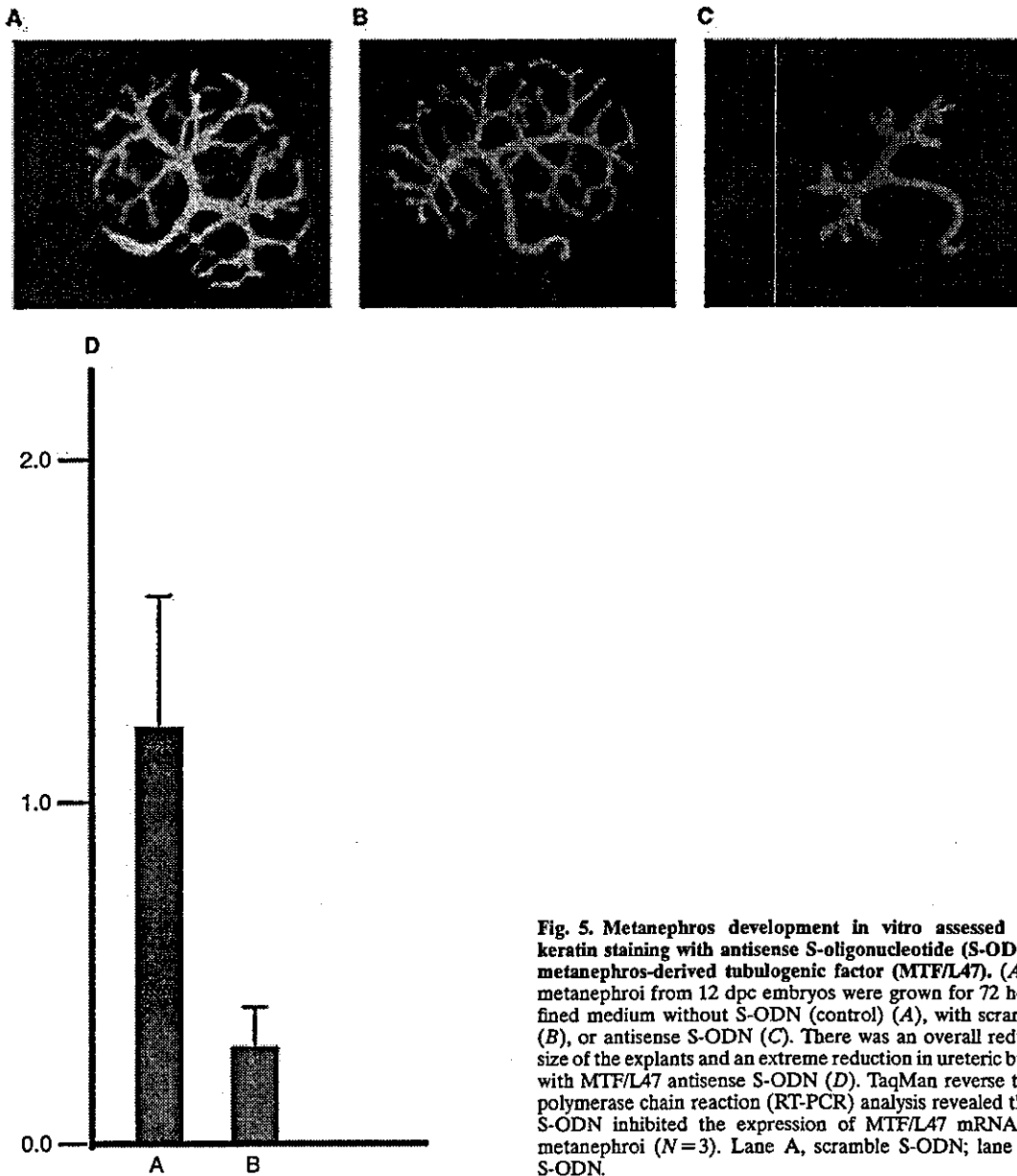


**Fig. 5. Metanephros development in vitro assessed by pan-cytokeratin staining with antisense S-oligonucleotide (S-ODN) of mouse metanephros-derived tubulogenic factor (MTF/L47).** (A) Explanted metanephroi from 12 dpc embryos were grown for 72 hours in a defined medium without S-ODN (control) (A), with scramble S-ODN (B), or antisense S-ODN (C). There was an overall reduction in the size of the explants and an extreme reduction in ureteric bud branching with MTF/L47 antisense S-ODN (D). TaqMan reverse transcription-polymerase chain reaction (RT-PCR) analysis revealed that antisense S-ODN inhibited the expression of MTF/L47 mRNA in cultured metanephroi ( $N=3$ ). Lane A, scramble S-ODN; lane B, antisense S-ODN.

of epithelial cells downstream of growth factors. For example, HGF-mediated induction of branching processes in Madin Darby canine kidney (MDCK) cells can be modulated by multiple phosphorylation mechanisms, including PKC, PKA, and  $Ca^{2+}$ /calmodulin-dependent kinase [19].

PKC is involved in regulation of the growth and differentiation of many organs during development, and expression of PKC- $\alpha$ , - $\delta$ , and - $\zeta$  in the developing kidney has been detected by Northern blot analysis [20]. Ceramide, a sphingolipid implicated in cellular differentiation, growth inhibition, and apoptosis, has been shown to selectively interact with PKC- $\alpha$  and - $\delta$

in mesangial cells, and to be capable of inducing apoptosis by PKC- $\alpha$  inactivation [21]. Addition of ceramide to metanephric organ culture has been found to induce apoptosis and impair nephron formation [4].

Although these previous studies pointed to a role of PKC in renal development, the mediator of the PKC responses in renal development was unknown. In this study, we confirmed not only decreased branching in response to ceramide, but increased branching in response to PKC activation by PMA, suggesting the possible existence of a PKC-related gene that regulates branching morphogenesis. This led to the identification of a novel gene, MTF/L47, by the differential display technique.

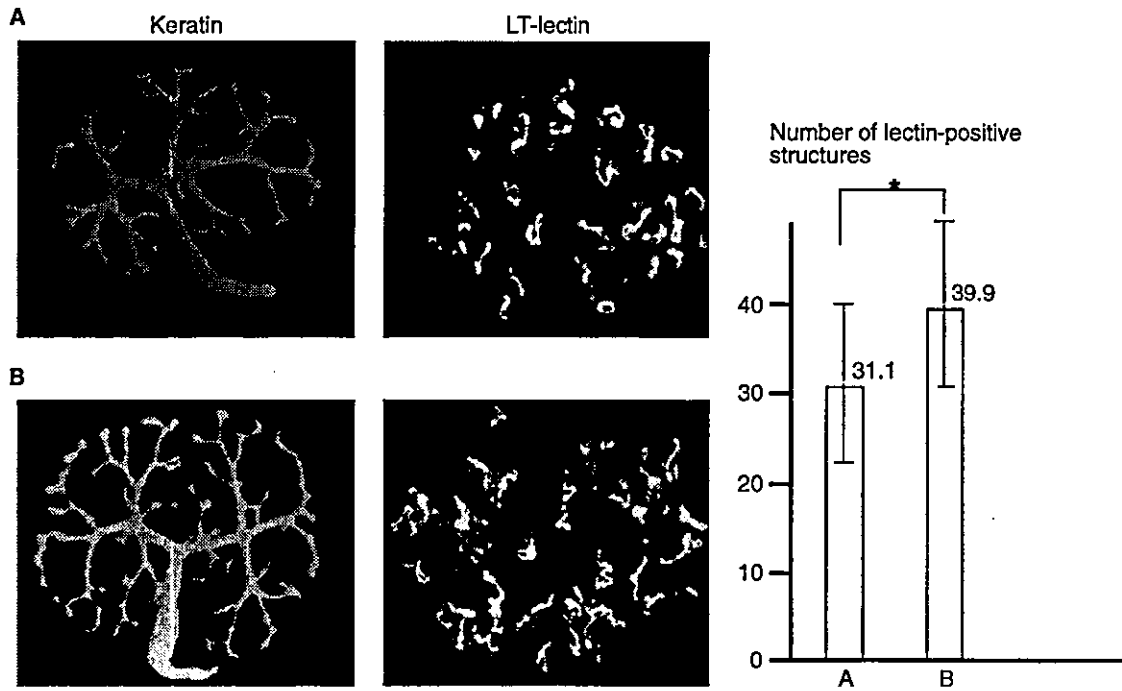


Fig. 6. Metanephros development in vitro assessed by pancyto-keratin staining and LT-lectin staining with recombinant mouse metanephros-derived tubulogenic factor (MTF/L47) protein. Explanted metanephroi from 12 dpc embryos were grown for 72 hours in a defined medium with or without recombinant MTF/L47. Ureteric bud branching was promoted in the explants treated with recombinant MTF/L47 protein (B) compared with the control (A). The explants treated with recombinant MTF/L47 protein contained more LT-lectin-positive structures (B) than the control (A). The number of LT-lectin-positive structures increased from 31.0 per metanephros to 39.9 per metanephros in response to recombinant protein (N=9).

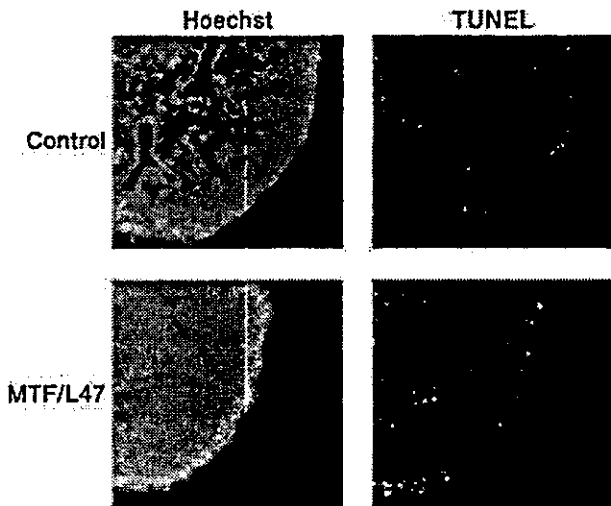


Fig. 7. Apoptosis of metanephroi cultured with and without recombinant mouse metanephros-derived tubulogenic factor (MTF/L47) protein. There was no significant difference in apoptosis between metanephroi cultured with and without recombinant MTF/L47 protein as assessed TUNEL assay.

RT-PCR analysis showed that MTF/L47 mRNA is strongly expressed in the embryonic kidney at days 12 and 16, coinciding with the timing of tubulogenesis and glomerulogenesis.

Metanephros organ culture provides a good model for investigating kidney morphogenesis and branching. GDNF significantly increased branching morphogenesis of the E11.5 metanephros and it induced the formation of ectopic ureteric buds from the base of the bud and from the Wolffian duct by enhancing cell survival, and possibly by increasing proliferation in organ culture [22]. The data from the sequence analysis of MTF/L47 suggested that it was a soluble protein because almost all the amino acids contained in MTF were hydrophilic. We then added the recombinant MTF/L47 protein to organ cultures. Addition of the antisense ODN of MTF/L47 decreased branching of the ureteric bud, whereas addition of recombinant MTF/L47 increased it. MTF/L47 may have the ability to promote branching morphogenesis of renal epithelial cells, the same as GDNF.

Overexpression of PKC-delta and PKC-epsilon induces apoptosis, while overexpression of PKC-alpha inhibits the onset of apoptosis via phosphorylation of Akt on serine 473 [23]. The fact that the metanephroi cultured with recombinant MTF/L47 protein were larger than the controls also suggested that the predominant effect of MTF/L47 might be to prevent apoptosis. However, the metanephroi cultured with recombinant MTF/L47 protein showed no marked change in apoptosis as assessed by the TUNEL method in organ culture. PKC has also been

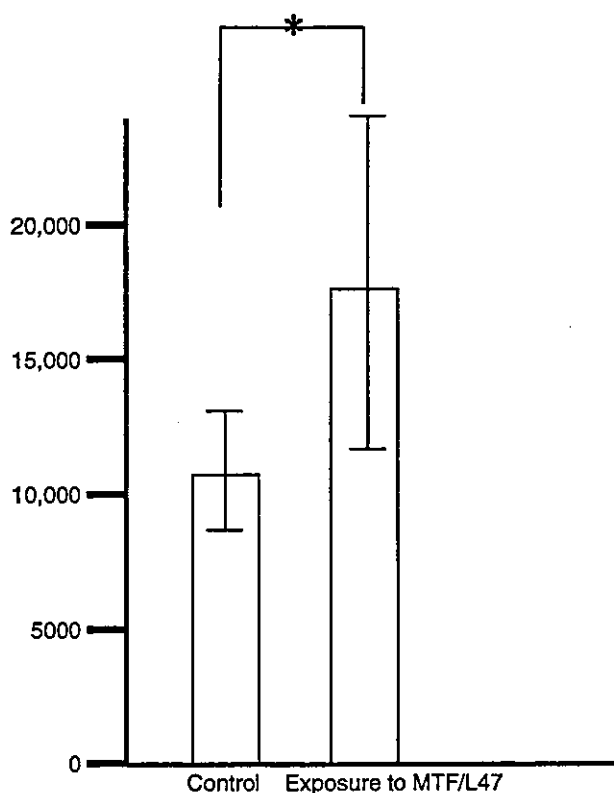


Fig. 8. Cell proliferation in metanephroi cultured with and without recombinant mouse metanephros-derived tubulogenic factor (MTF/L47) protein. [<sup>3</sup>H]-thymidine-associated incorporation was measured in metanephroi cultured with and without recombinant MTF/L47. [<sup>3</sup>H]-thymidine-associated incorporated radioactivity was higher in kidneys exposed to MTF/L47 recombinant protein ( $N = 18$ ). \* $P < 0.05$ .

implicated in the proliferation of several types of cells, and both PKC activation by phorbol ester or lead acetate and PKC- $\alpha$  overexpression increase DNA synthesis [24–26]. In this study, an increase in thymidine uptake was observed in metanephroi cultured with recombinant MTF/L47 protein. Thus, MTF/L47 may play a role in the cell proliferative function of PKC.

A recent cDNA sequence analysis has shown MTF/L47 to be a homologue of mitochondrial ribosomal protein L47 [27]. Nearly half of the ribosomal protein transcripts were found to undergo statistically significant nerve growth factor (NGF)-promoted alteration in relative abundance, with changes up to fivefold in PC12 cells [28]. PKC may regulate many ribosomal protein transcriptions, similar to NGF. Some ribosomal proteins undergo changes in expression in response to various tissue conditions. Heparin/HS interacting protein (HIP/RPL29) is a small, highly basic, heparin/heparan sulfate interacting protein, identical to ribosomal protein L29, and its expression depends on the growth/differentiation state of the luminal epithelium [29]. Recombinant human HIP/L29 decreased basic FGF-induced proliferation in

fibroblasts from normal gingiva by inhibiting basic FGF stimulation of mitogen-activated protein kinase (MAPK) p44 (Erk-1) [30], and apoptosis-related protein [death-associated proteins (DAP3)] has been shown to be a ribosomal protein [31, 32]. Thus, there may be other ribosomal proteins that control not only apoptosis but also cascades of growth factors, the same as HIP/PRL29, and MTF/L47 may be one of them.

The pathway by which MTF/L47 induced cell proliferation in the metanephroi was not identified in the present study, and it is also unknown whether endogenous MTF/L47 produced the by metanephros is secreted into the extracellular fluid. The precise characteristics of this protein should be determined in future studies.

## CONCLUSION

We identified a novel gene, *MTF/L47*, by differential display and demonstrated that MTF/L47 is capable of regulating kidney development by controlling cell proliferation.

## ACKNOWLEDGMENTS

This research was supported in part by grants from the Ministry of Education, Science and Culture in Japan to T.A., and from Health Science Research Grants from the Ministry of Health and Welfare to M.H.

Reprint requests to Matsuhiko Hayashi, M.D., Department of Internal Medicine, Keio University School of Medicine, 35 Shinanomachi, Shinjuku-ku, Tokyo, 160-8582, Japan.  
E-mail: matuhiko@sc.itc.keio.ac.jp

## REFERENCES

1. SAXEN L, LEHTONEN E: Embryonic kidney in organ culture. *Differentiation* 36:2–11, 1987
2. SPOSI NM, BOTTERO L, COSSU G, et al: Expression of protein kinase C genes during ontogenic development of the central nervous system. *Mol Cell Biol* 9:2284–2288, 1989
3. LIVINGSTON BT, WILT FH: Phorbol esters alter cell fate during development of sea urchin embryos. *J Cell Biol* 119:1641–1648, 1992
4. SERLACHUS E, SVENNILSON J, SCHALLING M, et al: Protein kinase C in the developing kidney: Isoform expression and effects of ceramide and PKC inhibitors. *Kidney Int* 52:901–910, 1997
5. ARAKI T, SARUTA T, OKANO H, et al: Caspase activity is required for nephrogenesis in the developing mouse metanephros. *Exp Cell Res* 243:423–429, 1999
6. LI Z, STUART RO, QIAO J, PAVLOVA A, et al: A role for Timeless in epithelial morphogenesis during kidney development. *Proc Natl Acad Sci USA* 97:10038–10043, 2000
7. KANWAR YS, LIU ZZ, KUMAR A, et al: D-glucose-induced dysmorphogenesis of embryonic kidney. *J Clin Invest* 98:2478–2488, 1996
8. BARROS EJ, SANTOS OF, MATSUMOTO K, et al: Differential tubulogenic and branching morphogenetic activities of growth factors: Implications for epithelial tissue development. *Proc Natl Acad Sci USA* 92:4412–4416, 1995
9. CANTLEY LG, BARROS EJ, GANDHI M, et al: Regulation of mitogenesis, motogenesis, and tubulogenesis by hepatocyte growth factor in renal collecting duct cells. *Am J Physiol* 267(2 Pt. 2):F271–F280, 1994
10. MONTESANO R, MATSUMOTO K, NAKAMURA T, et al: Identification of a fibroblast-derived epithelial morphogen as hepatocyte growth factor. *Cell* 67:901–908, 1991

11. SAKURAI H, BARROS EJ, TSUKAMOTO T, *et al*: An in vitro tubulogenesis system using cell lines derived from the embryonic kidney shows dependence on multiple soluble growth factors. *Proc Natl Acad Sci USA* 94:6279–6284, 1997
12. PICHEL JG, SHEN L, SHENG HZ, *et al*: Defects in enteric innervation and kidney development in mice lacking GDNF. *Nature* 382:73–76, 1996
13. ROGERS SA, RYAN G, HAMMERMAN MR: Insulin-like growth factors I and II are produced in the metanephros and are required for growth and development in vitro. *J Cell Biol* 113:1447–1453, 1991
14. LIU ZZ, KUMAR A, WALLNER EI, *et al*: Trophic effect of insulin-like growth factor-I on metanephric development: relationship to proteoglycans. *Eur J Cell Biol* 65:378–391, 1994
15. PARTANEN AM: EGF receptors in the development of epitheliomesenchymal organs. *Mol Reprod Dev* 27:60–65, 1990
16. PUGH JL, SWEENEY WE JR, AVNER ED: Tyrosine kinase activity of the EGF receptor in murine metanephric organ culture. *Kidney Int* 47:774–781, 1995
17. PERANTONI AO, DOVE LF, KARAVANOVA I: Basic fibroblast growth factor can mediate the early inductive events in renal development. *Proc Natl Acad Sci USA* 92:4696–4700, 1995
18. VUKICEVIC S, KOFF JB, LUYTEN FP, *et al*: Induction of nephrogenic mesenchyme by osteogenic protein 1 (bone morphogenetic protein 7). *Proc Natl Acad Sci USA* 93:9021–9026, 1996
19. SANTOS OF, MOURA LA, ROSEN EM, *et al*: Modulation of HGF-induced tubulogenesis and branching by multiple phosphorylation mechanisms. *Dev Biol* 159:535–548, 1993
20. OSTLUND E, MENDEZ CF, JACOBSSON G, *et al*: Expression of protein kinase C isoforms in renal tissue. *Kidney Int* 47:766–773, 1995
21. HUWILER A, FABBRO D, PFEILSCHIFTER J: Selective ceramide binding to protein kinase C-alpha and -delta isoenzymes in renal mesangial cells. *Biochemistry* 37:14556–14562, 1998
22. TOWERS PR, WOOLF AS, HARDMAN P: Glial cell line-derived neurotrophic factor stimulates ureteric bud outgrowth and enhances survival of ureteric bud cells in vitro. *Exp Nephrol* 6:337–351, 1998
23. LI W, ZHANG J, FLECHNER L, *et al*: Protein kinase C-alpha overexpression stimulates Akt activity and suppresses apoptosis induced by interleukin 3 withdrawal. *Oncogene* 18:6564–6572, 1999
24. ITOH H, YAMAMURA S, WARE JA, *et al*: Differential effects of protein kinase C on human vascular smooth muscle cell proliferation and migration. *Am J Physiol Heart Circ Physiol* 281:H359–H370, 2001
25. LU H, GUIZZETTI M, COSTA LG: Inorganic lead stimulates DNA synthesis in human astrocytoma cells: Role of protein kinase Calpha. *J Neurochem* 78:590–599, 2001
26. MANDIL R, ASIKENAZI E, BLASS M, *et al*: Protein kinase Calpha and protein kinase C delta play opposite roles in the proliferation and apoptosis of glioma cells. *Cancer Res* 61:4612–4619, 2001
27. KOC EC, BURKHART W, BLACKBURN K, *et al*: The large subunit of the mammalian mitochondrial ribosome. Analysis of the complement of ribosomal proteins present. *J Biol Chem* 276:43958–43969, 2001
28. ANGELASTRO JM, TOROCSIK B, GREENE LA: Nerve growth factor selectively regulates expression of transcripts encoding ribosomal proteins. *BMC Neurosci* 3:3, 2002
29. KIRN-SAFRAN CB, JULIAN J, FONGEMIE JE, *et al*: Changes in the cytologic distribution of heparin/heparan sulfate interacting protein/ribosomal protein L29 (HIP/RPL29) during in vivo and in vitro mouse mammary epithelial cell expression and differentiation. *Dev Dyn* 223:70–84, 2002
30. TA TV, BARANIAK D, JULIAN J, *et al*: Heparan sulfate interacting protein (HIP/L29) negatively regulates growth responses to basic fibroblast growth factor in gingival fibroblasts. *J Dent Res* 81:247–252, 2002
31. LEVY-STRUMPF N, KIMCHI A: Death associated proteins (DAPs): From gene identification to the analysis of their apoptotic and tumor suppressive functions. *Oncogene* 17:3331–3340, 1998
32. CAVDAR KOC E, RANASINGHE A, BURKHART W, *et al*: A new face on apoptosis: Death-associated protein 3 and PDCD9 are mitochondrial ribosomal proteins. *FEBS Lett* 492:166–170, 2001

## Genetic Polymorphism of *NPHS1* Modifies the Clinical Manifestations of Ig A Nephropathy

Ichiei Narita, Shin Goto, Noriko Saito, Jin Song, Daisuke Kondo, Kentaro Omori, Hiroshi Kawachi, Fujio Shimizu, Minoru Sakatsume, Mitsuhiro Ueno, and Fumitake Gejyo

*Division of Clinical Nephrology and Rheumatology (IN, SG, NS, JS, DK, KO, MS, MU, FG), and Department of Cell Biology (HK, FS), Institute of Nephrology, Niigata University Graduate School of Medical and Dental Sciences, Asahimachi-dori, Niigata, Japan*

**SUMMARY:** Nephrin, the molecule responsible for congenital nephrotic syndrome of Finnish type, is crucial in maintaining the glomerular filtration barrier. Recently, its complete gene structure and common gene polymorphisms in its exons have been reported, although the functional and clinical significance of these polymorphisms has not yet been elucidated. We investigated a possible association of the *NPHS1* polymorphisms with the development of Ig A nephropathy (IgAN), as well as the clinical and histologic manifestations in IgAN. A total of 464 Japanese subjects, including 267 patients with histologically proven IgAN and 197 healthy controls with normal urinalysis, were genotyped for the *NPHS1* G349A, G2289A, and T3315C polymorphisms. The frequencies of the genotypes, alleles, and estimated haplotypes of *NPHS1* polymorphisms were no different between patients with IgAN and the controls. Within the IgAN group, patients carrying at least one G allele of G349A tended to present with more proteinuria, lower renal function, and more severe histopathologic injury than those with the AA genotype, although the time from the first urinary abnormality to the renal biopsy was no different between both groups. The logistic regression analysis indicated that even after adjusting for the effect of proteinuria and hypertension the GG genotype of *NPHS1* G349A was an independent risk factor for the deteriorated renal function at the time of diagnosis. This study suggests that the *NPHS1* G349A polymorphism may be associated with heavy proteinuria and a decline in renal function in patients with IgAN. (*Lab Invest* 2003, 83:1193–1200).

Ig A nephropathy (IgAN) is one of the major causes of end-stage renal disease (ESRD) and the most common form of primary glomerulonephritis among patients undergoing renal biopsy throughout the world (Maisonneuve et al, 2000). It is characterized by mesangial proliferative glomerulonephritis with predominant deposits of IgA in the mesangial area. The actuarial renal survival in Japanese patients with IgAN at 10 years and 20 years is assumed to be 85% and 61%, respectively, from the time when the first renal abnormalities are detected (Koyama et al, 1997). Familial clustering of IgAN and interindividual differences in the clinical course suggests that genetic factors may contribute to both the development and progression of this disease (Galla, 2001; Hsu et al, 2000). It has been well documented that impairment of renal function, severe proteinuria, and arterial hypertension

at the time of diagnosis are the strongest and most reliable clinical predictors of progression to ESRD (D'Amico, 2000; Koyama et al, 1997).

The nephrin gene, *NPHS1* (AF035835), has recently been identified as the gene responsible for congenital nephrotic syndrome of the Finnish type (NPH1) (Kesätila et al, 1998), an autosomal recessive disorder characterized by the onset of nephrotic syndrome, which usually occurs before 3 months of age (Hallman et al, 1956). NPH1 previously resulted in death before age 2 years, but it can now be treated by kidney transplantation, without the development of extrarenal symptoms (Holmberg et al, 1995). The *NPHS1* gene consists of 29 exons spanning 26 kb in the chromosomal region 19q13.1 (Mannikko et al, 1995). In the kidney nephrin expression is observed only in visceral epithelial cells of the glomeruli, indicating its importance in the development or maintenance of the glomerular filtration barrier (Holthofer et al, 1999). In fact an mAb (mAb 5–1–6), which reacts with the slit diaphragm, induces a massive proteinuria (Orikasa et al, 1988), and the antigenic molecule recognized by mAb 5–1–6 has been identified as nephrin (Kawachi et al, 2000). The complete genomic structure for *NPHS1* was reported, and a total of 50 mutations in the coding region of *NPHS1* or the immediate 5'-flanking region have been identified in patients with NPH1 (Lenkkeri et al, 1999). In addition to these mutations, several sequence variants were published in Caucasian

DOI: 10.1097/01.LAB.0000080600.49276.31

Received April 21, 2003.

This work was supported in part by health and labor science research grants for research on specific diseases from the Ministry of Health, Labour, and Welfare (to FG); and by a Grant-in-Aid for Scientific Research (No. 11671032) from the Ministry of Education, Culture, Sports, Science, and Technology of Japan (to IN).

Address reprint requests to: Dr. Ichiei Narita, Division of Clinical Nephrology and Rheumatology, Niigata University Graduate School of Medical and Dental Sciences, 757, Asahimachi-dori, Niigata, 951–8510, Japan.  
E-mail: naritai@med.niigata-u.ac.jp

(Beltcheva et al, 2001), as well as in Japanese control individuals (Hirakawa et al, 2002) (an online database of Japanese single nucleotide polymorphisms [SNPs] can be found at <http://snp.ims.u-tokyo.ac.jp>). Although the functional significance of these gene polymorphisms remains unclear, it might be important to explore the phenotypic consequences imposed by the *NPHS1* polymorphisms, not only in congenital nephrotic syndrome, but also in common glomerular diseases.

In this study to investigate the possible role of the *NPHS1* polymorphism on the development of IgAN, as well as on the clinical manifestations of the disease, we performed a case control study for the *NPHS1* G349A, G2289A, and T3315C polymorphisms in patients with IgAN and healthy controls in the Japanese population.

## Results

In total we genotyped 464 subjects, which consisted of 267 patients with histologically proven IgAN and 197 healthy controls who were genotyped for *NPHS1* G349A, G2289A, and T3315C. Table 1 lists the genotype distributions and the allele frequencies of these gene polymorphisms in both groups. The expected frequencies of the genotypes in both groups, under the assumption of Hardy-Weinberg equilibrium, did

not differ from the observed genotype frequencies. No difference was recognized in the genotype and allele frequency between the patients with IgAN and the healthy controls without any history of renal disease or hypertension. Table 1 also shows estimated frequencies of four major haplotypes for the three SNPs loci in *NPHS1*. The frequencies of these haplotypes were no different between IgAN patients and controls. A complete linkage disequilibrium was observed between the loci 349 and 2289 ( $D' = 1.0000$ ,  $p < 0.0001$ ), but not between 3315 and the other two loci (349 and 3315,  $D' = 0.6513$ ,  $p = 0.0732$ ; 2289 and 3315,  $D' = 0.7480$ ,  $p = 0.1030$ ).

Clinical characteristics of patients with IgAN at the time of renal biopsy are listed in Table 2. The comparisons shown in this table were made between patients with the homozygote of *NPHS1* 349A ( $n = 102$ ) and those with either the heterozygote or homozygotes of 349G ( $n = 165$ ). There was no difference in the gender, age, body mass index, time from the first urine abnormality to renal biopsy, and blood pressure at the time of renal biopsy between the two groups. Urinary protein excretion at the time of renal biopsy in patients with the AA genotype tended to be less in comparison to patients with the other genotypes, but the difference was not statistically significant. The incidence of nephrotic range proteinuria (NS; urinary protein of

**Table 1. Genotype Distributions and Allele Frequencies of Gene Polymorphisms in Patients with Histologically Proven IgAN and Healthy Controls**

Genotype			IgAN	Control	$\chi^2$	p Value
			N = 267	N = 197		
G349A	GG		37	34	1.210	0.5460
	GA		128	87		
	AA		102	76		
G2289A	GG		178	143	2.130	0.3447
	GA		82	51		
	AA		7	3		
T3315C	TT		171	124	1.676	0.4326
	TC		82	67		
	CC		14	6		
Allele			N = 534	N = 394		
G349A	G		0.378	0.393	0.219	0.638
	A		0.622	0.607		
G2289A	G		0.821	0.860	2.687	0.101
	A		0.179	0.140		
T3315C	T		0.793	0.802	0.711	0.137
	C		0.207	0.198		
Haplotype estimated			N = 534	N = 394		
G349A	G2289A	T3315C				
A	G	C	0.136	0.156		
A	G	T	0.483	0.442		
G	A	T	0.145	0.146		
G	G	T	0.166	0.188		
Others			0.070	0.068	1.841	0.765

IgAN, Ig A nephropathy.

Table 2. Clinical Characteristics of Patients with Ig A Nephropathy

	All patients N = 267	Genotype of <i>NPHS1</i> G349A		p Value	$\chi^2$
		AA N = 102	GA/GG N = 165		
Gender (male %)	48.5	46.1	50.0	NS	
Age (year)	37.1 ± 13.4	36.9 ± 12.6	37.2 ± 13.8	NS	
Body mass index	22.56 ± 3.20	22.89 ± 3.52	22.34 ± 3.69	NS	
Time from the first urine abnormality to renal biopsy (month)	57.6 ± 67.7	56.3 ± 55.7	58.4 ± 74.5	NS	
Urinary protein excretion (g/day)	1.3 ± 1.3	1.1 ± 0.9	1.5 ± 1.5	NS	
Incidence of nephrotic range proteinuria (%)	7.9	2.0	11.5	0.0088	6.858
Serum creatinine (mg/dl)	1.0 ± 0.9	1.0 ± 1.3	1.1 ± 0.6	0.0333	
Creatinine clearance (ml/min)	87.5 ± 32.3	91.7 ± 31.2	84.9 ± 32.8	0.0223	
Incidence of advanced GN (%)	29.2	17.6	36.4	0.0012	10.477
Blood pressure (mmHg)					
Systolic	128.0 ± 18.6	129.1 ± 19.5	127.4 ± 18.1	NS	
Diastolic	77.1 ± 13.9	78.4 ± 14.1	76.4 ± 13.8	NS	
Incidence of hypertension (%)	37.8	36.3	38.8	NS	
ACE-I or ARB administration (%)	8.6	9.8	7.9	NS	

ACE-I, angiotensin-converting enzyme inhibitor; ARB, angiotensin-II receptor blocker; GN, glomerulonephritis.

more than 3.5 g/day) was significantly higher in patients with at least one G allele of the *NPHS1* G349A polymorphism.

The level of serum creatinine at the time of renal biopsy was lower and the 24-hour creatinine clearance (Ccr) was higher in patients with the AA genotype than those with the GA or GG genotype. Moreover, the incidence of advanced glomerulonephritis (GN) was significantly higher in patients with the GA or GG genotypes of the G349A polymorphism than those with the AA genotype. Table 3 lists the frequencies of alleles for the *NPHS1* polymorphisms in IgAN patients with or without NS, and those with or without advanced GN. Again, the G349A polymorphism was significantly associated with both NS and advanced GN. In contrast, T3315C was not associated with NS or advanced GN. In the haplotype analysis, in which haplotype frequencies for the G349A and G2289A loci

were estimated in IgAN patients, the haplotype A-G was observed more frequently in the patients without NS and in those without advanced GN (Table 3). The T3315C polymorphism was not included in the haplotype estimation because this locus was not in linkage disequilibrium with the other two loci and was not associated with NS nor advanced GN.

The G349A in the *NPHS1* were likely to be associated with both urinary protein excretion and renal function at the time of renal biopsy. However, these two clinical phenotypes were actually correlated to each other (data not shown). Therefore, to investigate whether the *NPHS1* polymorphism affected the renal function at the time of renal biopsy independently of urinary protein excretion, the multivariate logistic regression analysis was used (Table 4). Because not all of the patients could be unequivocally assigned to have a particular haplotype and because the G349A

Table 3. Frequencies of Alleles for the *NPHS1* Polymorphisms in Ig A Nephropathy Patients with or without Nephrotic Syndrome and Those with or without Advanced GN

SNP	Allele	Nephrotic syndrome		$\chi^2$	p Value	Advanced GN		$\chi^2$	p Value
		Yes N = 42	No N = 492			Yes N = 156	No N = 378		
G349A	G	0.524	0.366	4.105	0.0428	0.474	0.339	8.651	0.0033
	A	0.476	0.634			0.526	0.661		
G2289A	G	0.714	0.829	3.470	0.0625	0.795	0.831	0.961	0.3270
	A	0.286	0.171			0.205	0.169		
T3315C	T	0.738	0.799	0.871	0.3506	0.769	0.804	0.827	0.3631
	C	0.262	0.201			0.231	0.196		
Haplotype of G349A and G2289A									
	A-G	0.476	0.634	4.105	0.0428	0.526	0.662	8.651	0.0033
	G-A	0.286	0.171	3.470	0.0625	0.208	0.169	0.961	0.3270
	G-G	0.238	0.195	0.449	0.5027	0.266	0.169	6.929	0.0085

GN, glomerulonephritis; SNP, single nucleotide polymorphism.

Table 4. Multiple Logistic Regression Analysis for a Deteriorated Renal Function at the Time Renal Biopsy

	$\chi^2$	<i>p</i> Value	Odds ratio	95% CI
Urinary protein excretion			Referent	
<1.0 g/day				
1.0 to 3.5 g/day	4.205	0.0403	1.969	1.030–3.763
>3.5 g/day	10.443	0.0012	7.315	2.188–24.456
Hypertension				
No			Referent	
Yes	13.677	0.0002	3.194	1.726–5.911
Genotype of <i>NPHS1</i> G349A				
AA			Referent	
AG	3.560	0.0452	1.982	1.032–4.033
GG	6.341	0.0118	3.299	1.303–8.354

polymorphism was most significantly associated with a deteriorated renal function, the G349A genotype was included in the multivariate analysis. In this analysis, the *NPHS1* G349A genotype was found to be an independent risk factor for advanced GN at the time of renal biopsy after adjusting for the effect of urinary protein excretion and hypertension. The odds ratios for the deteriorated renal function in patients with the AG or GG genotype versus those with AA as the reference were 1.982 (95% confidence interval, 1.032

to 4.033,  $\chi^2 = 3.560$ ,  $p = 0.0452$ ) and 3.299 (95% confidence interval, 1.303 to 8.354,  $\chi^2 = 6.341$ ,  $p = 0.0118$ ), respectively.

Next, any possible associations between the *NPHS1* genotype and histopathologic findings were investigated. Figure 1 shows the mean values of each histopathologic grading score in patients with the AA and AG/GG genotypes of *NPHS1* G349A. Patients carrying at least one G allele of the *NPHS1* G349A polymorphism had more severe histopathologic dam-

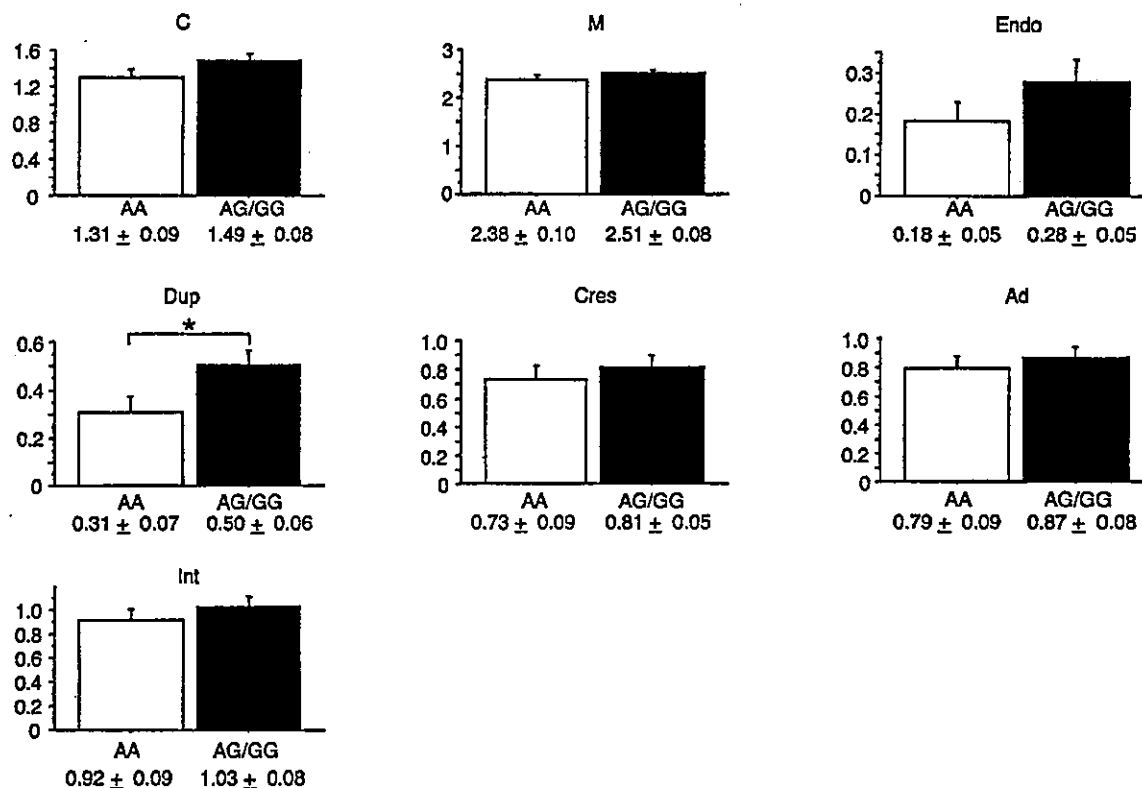


Figure 1.

Mean values of each histopathologic grading score in Ig A nephropathy patients with the AA (□) and AG/GG (■) genotypes of the *NPHS1* G349A polymorphism. Glomerular changes were scored for each glomerulus, and the average score of each was calculated. The scores for mesangial cell proliferation (C) and mesangial matrix increase (M) were graded into five grades ranging from 0 to 4. Other glomerular changes including endocapillary proliferation (Endo), duplication of glomerular basement membrane (Dup), crescent formation (Cres), and adhesion of tufts to Bowman's capsule (Ad), as well as tubulointerstitial lesions (Int), were graded 0 to 4 according to their incidence. Data are given as mean ± se, \* $p < 0.05$  by Mann-Whitney *U* test.



age, in particular, with respect to duplication of the glomerular basement membrane (AG/GG versus AA;  $0.51 \pm 0.70$  versus  $0.31 \pm 0.58$ ,  $p = 0.0307$ , by Mann-Whitney *U* test). No significant deference was observed between patients with the AA and AG/GG genotype in mean values of other histologic scores including mesangial cell proliferation, matrix increase, interstitial fibrosis, adhesion of glomerular tufts to Bowman's capsule, crescent formation, and endocapillary proliferation. However, patients with AG/GG genotype had a tendency to present with numerically higher grades in all respects to the histologic scores evaluated.

## Discussion

The results of the present study indicate a role of the genetic polymorphism of *NPHS1*, not in the development, but in the clinical manifestations of IgAN. The IgAN patients with the AG/GG genotypes of *NPHS1* G349A presented with more proteinuria, as well as an increased deterioration in renal function compared with those with AA genotypes. The results of the histopathologic assessments of the patients were in accordance with the clinical data. T3315C, which is 20-kb distant from G349A and 13kb from G2289A, was neither in linkage disequilibrium with the other two loci, nor associated with these clinical phenotypes. Although G349A and G2289A were in tight linkage disequilibrium, the significance of the association with heavy proteinuria and a deteriorated renal function was higher in G349A than in G2289A. This is thought to be due to the difference in allele frequency of these two SNPs, because it has been reported that in association studies SNPs with high allele frequencies are more statistically informative than those with low allele frequencies (Martin et al, 2000). In the haplotype analysis, the A-G haplotype was found to be a protective haplotype both for NS and for advanced GN. These clinical phenotypes are well known as significant risk factors for the progression to ESRD. However, to establish the prognostic significance of this gene polymorphism, a prospective randomized controlled study with a long-term observation is needed.

The filtration barrier of the glomerulus consists of a fenestrated endothelium, a layered glomerular basement membrane, and visceral epithelial cells, podocytes. Accumulating evidence indicates that the podocytes, with their primary and secondary foot processes, as well as the interpodocyte slit membranes, are the final glomerular barrier, which prevents the leakage of circulating macromolecules. Nephrin is a major molecule in the podocyte filtration slits. The remarkable regulation of nephrin-specific mRNA levels in experimental models has been reported (Luimula et al, 2000). More recently, a typical down-regulation of nephrin expression has been reported in the glomeruli of samples from patients with IgAN, membranous nephropathy, and membranoproliferative glomerulonephritis (Aaltonen et al, 2001; Kim et al, 2002; Wang et al, 2002). The predicted protein product of the *NPHS1* is a transmembrane protein with eight Ig-like

extracellular repeats and a uniquely structured intracellular domain (Kestila et al, 1998). The SNP G349A exists in exon three of the nephrin genes and is accompanied by the substitution of amino acid Lys for Glu117, whereas the other two SNPs do not cause amino acid substitution (Lenkkeri et al, 1999). Considering the pivotal role of the molecule in maintaining glomerular permselectivity, it is not surprising that the polymorphism has an association with urinary protein excretion and the incidence of heavy proteinuria caused by glomerular injury. Although, to date, there is no evidence available on the functional significance of the *NPHS1* polymorphism, an alteration in the function of the nephrin molecule, even to a minor extent, would lead to an alteration in both the physiologic and pathologic states of the glomerular podocyte. This in turn may affect the response of intrinsic renal cells to immunological injury such as IgAN, resulting in the clinical phenotype, whereas it would have no effect on the clinical phenotype in normal physiological conditions. There is also the possibility that other gene polymorphism, which is in linkage disequilibrium with the G349A in *NPHS1*, has a direct impact on expression or function of the gene and is responsible for the association observed in this study. We cannot provide the molecular mechanism by which the *NPHS1* polymorphism affects the renal function, as well as the urinary protein excretion. It might be argued that the association between the *NPHS1* polymorphism and the deteriorated renal function observed at the time of renal biopsy was a indirect consequence of the heavier proteinuria in patients with a 349G allele of the *NPHS1* polymorphism, because proteinuria is well known as a factor for renal damage. However, the result of the logistic regression analysis indicated the effect of the SNP on renal function was independent to proteinuria. This may suggest that nephrin plays an important role not only in maintaining the glomerular filtration barrier, but also in regulating podocyte function and its cell behavior in the disease state. It is crucial to clarify the functional significance of this genetic polymorphism especially on the podocyte function both in the normal physiological condition and in the inflammatory response.

Our recent investigation has demonstrated that podocyte injury accompanied by down-regulation of nephrin is one of the important factors in bringing on irreversible glomerular alterations (Morioka et al, 2001). It is possible that an alteration in the expression of nephrin in the pathologic state, which might be associated with the *NPHS1* polymorphism, is followed by more severe glomerular injury. The limitation of the present study is that we could not clarify the mechanism by which the *NPHS1* was associated with severe histologic injury and that we could not provide direct evidence for an association between the *NPHS1* polymorphism and the expression of nephrin protein in patients with IgAN. However, the histologic investigation in this study may support the possibility that the *NPHS1* polymorphism has a direct or specific effect on podocyte in the disease state.

We selected IgAN patients as the subjects of this investigation because they are the largest population of patients with an identical histologic disease entity. Moreover, the patients with IgAN in this study were diagnosed at a single center, and the records of their clinical data at the time of renal biopsy were available. The effect of the genetic polymorphisms in *NPHS1* on the clinical manifestations of glomerular disease observed in this study may not be specific to IgAN. It is rather likely that the gene polymorphism investigated in this study affects the clinical phenotypes in other types of glomerular diseases. Although, if no association is found with other disease groups, that may provide an important negative control. However, it is thought that small sample size groups with heterogeneous disease entities are inadequate for proving any negative or positive association between genotype and phenotype.

There is a possibility that the *NPHS1* polymorphism merely provides a fortunate marker of other differences in the genetic background that serves as genetic modifiers. A further large population-based and genome-wide study is necessary to clarify the genetic factors contributing to the development of IgAN, and this would be helpful in understanding the pathogenetic mechanism of IgAN as well as developing a new strategy for treatment of the disease.

Although further study is necessary to elucidate the functional significance of the *NPHS1* polymorphism on nephrin expression or podocyte function, the findings of this study support the important role of podocyte damage for developing and progression of glomerular injury in IgAN.

## Materials and Methods

### Patients

The protocol for the genetic study was approved by the ethics committee of the institution involved, and informed written consent for the genetic studies was obtained from all participants.

Genomic DNA of peripheral blood cells from 464 Japanese individuals including 267 patients with histologically confirmed IgAN was isolated using an automatic DNA isolation system (NA-1000, Kurabo, Osaka, Japan). Schönlein-Henoch purpura and secondary IgAN such as hepatic glomerulosclerosis were excluded from the analysis. Diagnosis of IgAN in all cases was based on a kidney biopsy that revealed the presence of dominant or co-dominant glomerular mesangial deposits of IgA as assessed by an immunofluorescence examination. The mean age at diagnosis was  $37.1 \pm 13.4$  (range from 9 to 74) years.

Clinical characteristics of the patients with IgAN, including gender, age, body mass index, duration of observation (in months), level of urinary protein excretion (g/day), serum creatinine (mg/dL), and Ccr (ml/min), were investigated before the start of any treatment. The time from the first urine abnormality to renal biopsy (month) was also recorded for 213 of the 267 patients, where the first episode of urine abnormality

(proteinuria or hematuria) could be clearly defined. Advanced GN was defined by a 24-hour CCr of  $< 70$  ml/min/1.73 m<sup>2</sup> body surface area. Hypertension was defined by the use of one or more antihypertensive medications and/or a blood pressure greater than or equal to 140 mmHg systolic or 90 mmHg diastolic. Only 23 of the 267 (8.6%) patients were administered angiotensin-converting enzyme inhibitors and/or angiotensin receptor antagonists before the diagnosis.

To provide a control for the local genotype frequency being examined, 197 Japanese volunteers (98 female and 99 male) with no history of renal disease or hypertension and with normal urinalysis were also recruited. The mean age of healthy controls was  $39.2 \pm 10.6$  years, and this was no different from that of the patients ( $p = 0.0817$ ).

### Determination of the Genotypes

After investigating the clinical characteristics from past medical records, genotypes for the *NPHS1* G349A, G2289A, and T3315C polymorphisms, which are located in exon 3, 17, and 25 of the gene, respectively, were independently determined in a double-blind fashion by allele specific oligonucleotide hybridization after PCR (PCR) using allele specific primers as shown in Table 5. These SNPs were selected for analysis because the frequencies of their minor alleles were more than 0.1 in a preliminary analysis, in which 100 healthy controls were genotyped. A DNA fragment containing the SNP region of the *NPHS1* was amplified by PCR, with two allele-specific sense primers and biotin-labeled antisense primers or vice versa, which were designed based on the published sequence (GenBank accession number AF035835). The second base from the 3'-end of the allele specific primer had each allele specific sequence, and the third base had an artificial mismatch sequence. The artificial mismatch was a mixture of nucleotides G or C to obtain the highest specificity in the following hybridization reaction. The reaction mixture in KOD plus buffer (25  $\mu$ l) contained 0.02  $\mu$ g of DNA, 5 pmol of each oligonucleotide primer, 0.2 mM each deoxynucleoside triphosphate, 0.9 mM MgSO<sub>4</sub>, and 1 unit of DNA polymerase (KOD plus, Toyobo, Osaka, Japan). The amplification protocol comprised of an initial denaturation at 94° C for 5 minutes; 35 cycles of denaturation at 95° C for 15 seconds, annealing at 65° C for 30 seconds, and an extension at 68° C for 30 seconds, with a final extension at 68° C for 2 minutes. Amplified DNA was denatured with NaOH, and then hybridized at 37° C for 30 minutes in hybridization buffer containing 30% formamide with allele-specific capture probes fixed to the bottom of the wells of a 96-well plate (Table 5). The wells were then washed thoroughly, and alkaline phosphatase-conjugated streptavidin added to each, before the plate was incubated at 37° C for 15 minutes. After washing each well thoroughly, 0.8 mM WST-1 (2-(4-iodophenyl)-3-(4-nitrophenyl)-5-(2,4-disulfophenyl)-2H-tetrazolium, monosodium salt) and 0.4 mM BCIP (5-bromo-4-chloro-3-indolyl phosphate p-toluidine

**Table 5. The Nucleotide Sequences of Primers for Allele Specific PCR and Hybridization Probes**

SNP		
G349A	Forward primer	5'-CCAGGTCGGCCGCTCXGA-3'
	Reverse primer	5'-CCAGGTCGGCCGCTCXAA-3'
	Hybridization probes	5'-biotin-CCATACCCAGGATGGAGAGGATCAC-3'
		5'-CCGCTCXGAGATGGGGCC-3
G2289A	Forward primer	5'-biotin-TGGATCCTCACCAGTCTCTCC-3'
	Reverse primer	5'-TGTGGACATAGTCTGCACTGXCG-3'
	Hybridization probes	5'-TGTGGACATAGTCTGCACTGXTG-3'
		5'-TCTGCACTGXCGATGCCAAT-3'
T3315C	Forward primer	5'-biotin-TGGCTCTCCTCATATTCGTTTC-3'
	Reverse primer	5'-CCTTCATCCTGGAAGGTXAG-3'
	Hybridization probes	5'-CTTCATCCTGGAAGGTXGG-3'
		5'-CTGGAAGGTXGAAGAGGACC-3'
		5'-CTGGAAGGTXGAAGAGGACC-3'

SNP, single nucleotide polymorphism.

salt), a substrate for alkaline phosphatase, were added and the colorimetry was measured.

To confirm the accuracy of the genotyping method, we also performed direct sequencing of the PCR products from 48 individuals (24 IgAN patients and 24 healthy controls randomly selected) using the TaqDNA polymerase cycle sequencing method. A BigDye Terminator Cycle Sequencing FS Kit was used according to the manufacturer's instruction (Perkin-Elmer, Foster City, California). The pairs of oligonucleotide primers as described previously were used for the bidirectional sequencing (Lenkkeri et al, 1999). An automated DNA sequencer (model ABI PRISM 310, Perkin-Elmer) was used for the analysis. The results of the direct sequencing were completely consistent with those of the allele-specific PCR method described above.

#### Histopathological Analysis

Histopathologic findings of kidney biopsy specimens of IgAN patients were classified according to the classification described previously (Suzuki et al, 1992). A single pathologist evaluated all specimens by light microscopy in a double-blind fashion. Glomerular changes were scored for each glomerulus, and the average score of each was calculated. The scores of cellular proliferation and the matrix increase in the mesangium were graded into five grades ranging from 0 (minimal change) to 4 (diffuse global marked). Other glomerular changes including endocapillary proliferation, duplication of glomerular basement membrane, crescent formation, and adhesion of tufts to Bowman's capsule as well as tubulointerstitial lesions were graded 0 to 4 according to their incidence. Grades 0 to 4 represent an incidence of the lesion in 0% to 4%, 5% to 24%, 25% to 49%, 50% to 74%, and 75% to 100% of cases, respectively.

#### Statistical Analysis

Haplotype frequencies for sets of alleles were estimated using ARLEQUIN software version 2.0, which

was based on a maximum-likelihood method. (Genetics and Biometry Laboratory, Department of Anthropology, University of Geneva, Geneva, Switzerland; <http://lgb.unige.ch/arlequin/>). Pair-wise linkage disequilibrium coefficients ( $D'$ ) were also calculated using ARLEQUIN version 2.0 and expressed as the  $D' = D/D$  max, according to Slatkin (Slatkin, 1994).

Statview 5.0 statistical software (Abacus Concepts, Inc., Berkeley, California) was used for statistical analyses on a Macintosh G4 computer. Chi-square analysis was used when comparing allele frequencies and categorical variables between the groups. Hardy-Weinberg equilibrium was tested by a Chi-square test with 1 *df*. The adjusted odds ratios and 95% confidence interval for advanced GN at the time of renal biopsy with multivariate factors were calculated using logistic regression analysis. Variables that achieved statistical significance ( $p < 0.05$ ) in the univariate analysis were subsequently included in a multivariate analysis using a stepwise forward logistic regression procedure and the effects of these covariates were expressed by an odds ratio. A  $p$  value of  $< 0.05$  was considered statistically significant.

#### Acknowledgements

A part of this study was presented at the 2002 American Society of Nephrology Renal Week, Philadelphia, Pennsylvania, and was published in abstract form (*J Am Soc Nephrol* 13:519A, 2002). The authors wish to thank Naofumi Imai, Keiko Yamagiwa, Noriko Ikeda, and Kumiko Furui for excellent technical assistance.

#### References

Aaltonen P, Luimula P, Astrom E, Palmén T, Gronholm T, Palojoki E, Jaakkola I, Ahoia H, Tikkanen I, and Holthofer H (2001). Changes in the expression of nephrin gene and protein in experimental diabetic nephropathy. *Lab Invest* 81:1185-1190.

- Beltcheva O, Martin P, Lenkkeri U, and Tryggvason K (2001). Mutation spectrum in the nephrin gene (NPHS1) in congenital nephrotic syndrome. *Hum Mutat* 17:368-373.
- D'Amico G (2000). Natural history of Idiopathic IgA nephropathy: Role of clinical and histological prognostic factors. *Am J Kidney Dis* 36:227-237.
- Galla JH (2001). Molecular genetics in IgA nephropathy. *Nephron* 88:107-112.
- Hallman N, Hjelt L, and Ahvenainen EK (1956). Nephrotic syndrome in newborn and young infants. *Ann Paediatr Fenn* 2:227-241.
- Hirakawa M, Tanaka T, Hashimoto Y, Kuroda M, Takagi T, and Nakamura Y (2002). JSNP: A database of common gene variations in the Japanese population. *Nucleic Acids Res* 30:158-162.
- Holmberg C, Antikainen M, Ronnholm K, Ala Houhala M, and Jalanko H (1995). Management of congenital nephrotic syndrome of the Finnish type. *Pediatr Nephrol* 9:87-93.
- Holthofer H, Ahola H, Solin ML, Wang S, Palmen T, Luimula P, Miettinen A, and Kerjaschki D (1999). Nephrin localizes at the podocyte filtration slit area and is characteristically spliced in the human kidney. *Am J Pathol* 155:1681-1687.
- Hsu SI, Ramirez SB, Winn MP, Bonventre JV, and Owen WF (2000). Evidence for genetic factors in the development and progression of IgA nephropathy. *Kidney Int* 57:1818-1835.
- Kawachi H, Kolke H, Kurihara H, Yaoita E, Orkasa M, Shia MA, Sakai T, Yamamoto T, Salant DJ, and Shimizu F (2000). Cloning of rat nephrin: Expression in developing glomeruli and in proteinuric states. *Kidney Int* 57:1949-1961.
- Kestila M, Lenkkeri U, Mannikko M, Lamerdin J, McCready P, Putaala H, Ruotsalainen V, Morita T, Nissinen M, Herva R, Kashtan CE, Peltonen L, Holmberg C, Olsen A, and Tryggvason K (1998). Positionally cloned gene for a novel glomerular protein—nephrin—is mutated in congenital nephrotic syndrome. *Mol Cell* 1:575-582.
- Kim BK, Hong HK, Kim JH, and Lee HS (2002). Differential expression of nephrin in acquired human proteinuric diseases. *Am J Kidney Dis* 40:964-973.
- Koyama A, Igarashi M, and Kobayashi M (1997). Natural history and risk factors for immunoglobulin A nephropathy in Japan. Research Group on Progressive Renal Diseases. *Am J Kidney Dis* 29:526-532.
- Lenkkeri U, Mannikko M, McCready P, Lamerdin J, Gribouval O, Niaudet PM, Antignac CK, Kashtan CE, Homberg C, Olsen A, Kestila M, and Tryggvason K (1999). Structure of the gene for congenital nephrotic syndrome of the Finnish type (NPHS1) and characterization of mutations. *Am J Hum Genet* 64:51-61.
- Luimula P, Ahola H, Wang SX, Solin ML, Aaltonen P, Tikkanen I, Kerjaschki D, and Holthofer H (2000). Nephrin in experimental glomerular disease. *Kidney Int* 58:1461-1468.
- Maisonneuve P, Agodoa L, Gellert R, Stewart JH, Buccianti G, Lowenfels AB, Wolfe RA, Jones E, Disney AP, Briggs D, McCredie M, and Boyle P (2000). Distribution of primary renal diseases leading to end-stage renal failure in the United States, Europe, and Australia/New Zealand: Results from an international comparative study. *Am J Kidney Dis* 35:157-165.
- Mannikko M, Kestila M, Holmberg C, Norio R, Ryyanen M, Olsen A, Peltonen L, and Tryggvason K (1995). Fine mapping and haplotype analysis of the locus for congenital nephrotic syndrome on chromosome 19q13.1. *Am J Hum Genet* 57:1377-1383.
- Martin ER, Lal EH, Gilbert JR, Rogala AR, Afshari AJ, Riley J, Finch KL, Stevens JF, Livak KJ, Slotterbeck BD, Silfer SH, Warren LL, Conneally PM, Schmechel DE, Purvis I, Pericak-Vance MA, Roses AD, and Vance JM (2000). SNPing away at complex diseases: Analysis of single-nucleotide polymorphisms around APOE in Alzheimer disease. *Am J Hum Genet* 67:383-394.
- Morioka Y, Kolke H, Ikezum Y, Ito Y, Oyanagi A, Gejyo F, Shimizu F, and Kawachi H (2001). Podocyte injuries exacerbate mesangial proliferative glomerulonephritis. *Kidney Int* 60:2192-2204.
- Orikasa M, Matsui K, Oite T, and Shimizu F (1988). Massive proteinuria induced in rats by a single intravenous injection of a monoclonal antibody. *J Immunol* 141:807-814.
- Slatkin M (1994). Linkage disequilibrium in growing and stable populations. *Genetics* 137:331-336.
- Suzuki S, Sato H, Kobayashi H, Takayama R, Maruyama Y, Ogino S, Ueno H, Inomata A, Nishi S, Saito T, and et al (1992). Comparative study of IgA nephropathy with acute and insidious onset. Clinical, laboratory and pathological findings. *Am J Nephrol* 12:22-28.
- Wang SX, Rastaldi MP, Patari A, Ahola H, Heikkila E, and Holthofer H (2002). Patterns of nephrin and a new proteinuria-associated protein expression in human renal diseases. *Kidney Int* 61:141-147.